

Low-loss terahertz superconducting plasmonics

This article has been downloaded from IOPscience. Please scroll down to see the full text article.

2012 New J. Phys. 14 115006

(<http://iopscience.iop.org/1367-2630/14/11/115006>)

View [the table of contents for this issue](#), or go to the [journal homepage](#) for more

Download details:

IP Address: 152.78.73.209

The article was downloaded on 27/11/2012 at 11:14

Please note that [terms and conditions apply](#).

Low-loss terahertz superconducting plasmonics

Anagnostis Tsiatmas¹, Vassili A Fedotov^{1,3},
F Javier García de Abajo^{1,2} and Nikolay I Zheludev¹

¹ Optoelectronics Research Centre and Centre for Photonic Metamaterials,
University of Southampton, Southampton SO17 1BJ, UK

² IQFR-CSIC Serrano 119, 28006 Madrid, Spain

E-mail: vaf@orc.soton.ac.uk

New Journal of Physics **14** (2012) 115006 (10pp)

Received 15 May 2012

Published 5 November 2012

Online at <http://www.njp.org/>

doi:10.1088/1367-2630/14/11/115006

Abstract. In the plasmonic regime, an electromagnetic wave bounded to the surface of a conductor can be confined to a region much smaller than its wavelength in free space. A major problem of plasmonic technology, however, is associated with large losses that these surface modes exhibit, intimately linked to Ohmic resistance of metals. In this work, we show that due to their dominant kinetic inductance, superconductors are intriguing yet natural plasmonic media capable of supporting low-loss plasmon waves with extreme confinement and the potential to serve as information carriers in compact terahertz data processing circuits.

The field of plasmonics, which deals with the optical properties of metallic nanostructures, is one of the most fascinating and fast-moving areas of photonics [1]. Its explosive growth in recent years has been driven by parallel advances in nano-fabrication technologies as well as a wealth of potential applications in areas ranging from bio-chemical sensing to solar power generation. The special interest in surface plasmon polaritons—bound oscillations of the electrons and light propagating along a metal surface—is based largely on the possibility that they may act as information carriers in highly integrated nanophotonic devices transforming the chip-scale data transport paradigm by bridging the gap between present-day electronic

³ Author to whom any correspondence should be addressed.



Content from this work may be used under the terms of the [Creative Commons Attribution-NonCommercial-ShareAlike 3.0 licence](https://creativecommons.org/licenses/by-nc-sa/3.0/). Any further distribution of this work must maintain attribution to the author(s) and the title of the work, journal citation and DOI.

and photonic technologies. The plasmonic response is also a dominant factor underpinning the functionality of photonic metamaterials [2]. However, the long-awaited promises of plasmonics are hampered by absorption losses, an inherited feature of metal-based waveguides supporting propagating plasmon signals. Losses also present a major problem in developing photonic metamaterial technologies. This challenge has brought about an intensive search for solutions such as plasmon-loss compensation with gain [3] and using new, better plasmonic materials [4].

Superconductors emerge as an intriguing low-loss alternative to plasmonic media. Low-dimensional plasma modes (analogous to bulk plasma excitations in metals) were predicted in thin superconducting wires [5] and layered superconductors [6, 7], and were experimentally demonstrated in thin superconducting films [8]. We now argue that recent developments in the field of superconducting metamaterials [9–13] and a clear demonstration of phenomena such as extraordinary transmission in perforated superconducting films [14, 15] bring about a practical proposition for propagating superconducting plasmons. We show that the latter are genuine bound surface modes similar to optical plasmons, which at THz frequencies can be guided with a nanometer-scale confinement propagating for tens of millimeters without noticeable attenuation.

Indeed, there are striking similarities between the electromagnetic response of metals at optical frequencies and superconductors at terahertz frequencies and below. In metals exposed to radio- and lower-frequency electromagnetic waves, the dynamics of a free electron is dominated by its ubiquitous collisions with atoms and lattice defects, as well as other free electrons taking place during each cycle of the driving field. As a result, the electron mean velocity and thus the strength of electrical currents induced by an external wave are proportional to the instantaneous value of the field with the constant of proportionality—the conductance—determined by the rate of such collisions. This is the regime described by Ohm’s law, in which the metal is characterized by a large value of the imaginary part of the metal permittivity and a smaller real part (see figure 1(a)). In contrast, at higher optical frequencies, electrons oscillate so rapidly that no collisions happen during at least one optical cycle: the collective dynamics of electron plasma is dominated by inertia of the carriers. Here we talk about the plasmonic regime: the displacement currents become important and the real part of the metal permittivity begins to dominate. In silver such a transition from Ohm’s law electrostatics to plasmonics occurs at frequencies above a few THz and extends into the infrared (IR) and the visible (see figure 1(a)). While the response of plasmonic metals is characterized by a dominant negative real part of the permittivity at optical frequencies, in the superconducting state such a behavior is found across most of the terahertz and sub-terahertz spectral domains (figure 1(b)). Indeed, the collective motion of ‘superconducting electrons’ joined in Cooper pairs experiences no scattering and proceeds freely through the lattice⁴. Their electrodynamic response, as in plasmonic metals, is thus determined by inertia. Moreover, the imaginary part of the permittivity is much lower than its real part. At higher frequencies, superconductors become lossy as the energy of the incident quanta is sufficient to break the Cooper pairs and destroy superconductivity. For example, for the high-temperature superconductor yttrium–barium–copper–oxide (YBCO), the spectral domain of plasmonic-like behavior extends from dc to a few THz.

Unfortunately, electromagnetic fields at the surface of superconductors are almost completely expelled from the medium, making plasmon-polariton-like excitations loosely bounded to the surface, weakly localized and thus unsuitable for waveguiding applications.

⁴ In the reverse analogy, plasmonic metals can be considered as behaving like high-frequency superconductors with the electrons in the macroscopically coherent state created through the coupling with incident light.

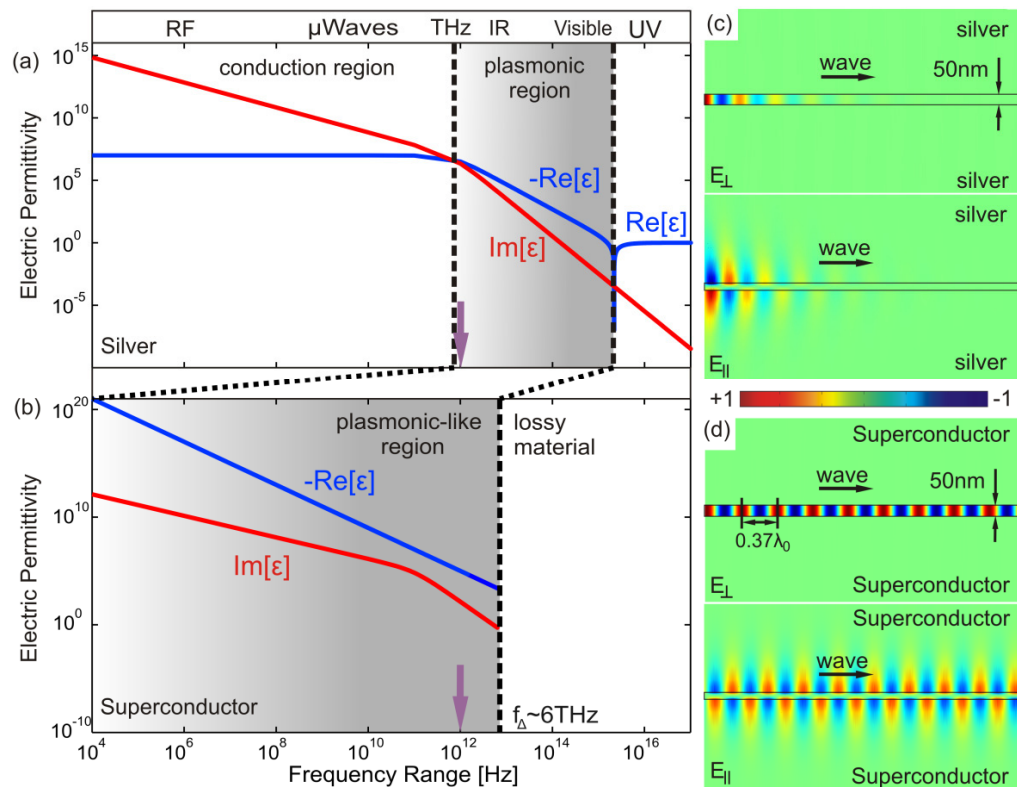


Figure 1. Metallic and superconducting plasmonic waveguides. The permittivity of silver ϵ , the Drude model (a), indicates plasmonic behavior in the IR and visible parts of the spectrum. A high-temperature superconductor, the two-fluid model (b), exhibits plasmonic-like behavior at terahertz frequencies and below. Here, f_{Δ} is the superconductor gap frequency. (c) and (d) Distribution of electric field in a TM wave propagating through silver (c) and superconducting (d) parallel-plate waveguides at 1 THz. E_{\parallel} and E_{\perp} are components of the wave electric field parallel and perpendicular to the propagation direction. In the silver waveguide the wave decays rapidly. The wave supported by the superconducting waveguide is ‘compressed’ (suitable for compact devices) and suffers negligible losses. Here $\lambda_0 = 0.3 \text{ mm}$ is the free-space wavelength.

For instance in YBCO at 1 THz, the surface wave extends into vacuum for tens of wavelengths and thus differs very little from a free-space plane wave propagating nearly parallel to the surface. Strong localization is a very desirable feature from the perspective of using superconducting plasmons as information carriers. It can be improved in superconducting films by significantly increasing the permittivity of the adjacent dielectric and/or at the expense of increased losses—either by using low-quality granular films [8] or operating at frequencies close to the bandgap [14].

We argue that there is a much better way to unlock the potential of superconducting plasmonics: namely, by using the waveguide configuration that literally squeezes the plasmonic field. This can be achieved by trapping the plasmonic field laterally between two superconducting surfaces of a parallel-plate waveguide with a sub-wavelength gap of just a few tens of nanometers (or using a nanometer-wide slot made in a thin superconducting film).

To prove our point, we simulated the propagation of electromagnetic fields at 1 THz in a 50 nm wide air gap between (i) two YBCO plates and (ii) two silver plates and compared the results for the two waveguide systems. In our simulation the superconductor is described using a well-known two-fluid model, which assumes the existence of two non-interacting electronic sub-systems contributing to the electromagnetic response of the superconductor at non-zero temperatures: superconducting electrons (Cooper pairs) with purely inertial dynamics of motion forming a super-current, and normal electrons participating in scattering and energy dissipation [16]. A generalized Drude model [17] is used to model the dielectric function of such a two-component electron plasma at frequencies below the superconductor gap frequency $2\Delta/\hbar$:

$$\varepsilon = \varepsilon' + i\varepsilon'' = 1 - \frac{\omega_s^2}{\omega^2} - \frac{\omega_n^2\tau^2}{\omega^2\tau^2 + 1} + i\frac{\omega_n^2\tau}{\omega(\omega^2\tau^2 + 1)}. \quad (1)$$

The second term in equation (1) represents the contribution from the non-dissipating super-current of Cooper pairs with plasma frequency $\omega_s = (N_s e^2 / m \varepsilon_0)^{1/2} = c / \lambda_L$, where λ_L is the London penetration depth, N_s is the density of superconducting electrons, m is their effective mass and ε_0 is the free-space permittivity. The third and fourth terms account for the normal electron plasma of resonant frequency $\omega_n = (N_n e^2 / m \varepsilon_0)^{1/2}$, where N_n is the density of normal electrons and τ is the relaxation time. The balance between densities of the superconducting and normal electrons is described by the empirical Gorter–Casimir relation $N_s = N[1 - (T/T_c)^4]$, where N is the temperature-independent total density of free carriers, while $N_n = N - N_s$ [15]. We choose the parameters in the superconductor model to describe $\text{YBa}_2\text{Cu}_3\text{O}_7$ with $T_c = 88$ K and $N = 1.255 \times 10^{27} \text{ m}^{-3}$. At $T = T_c$ the normal electron plasma frequency has the value $\omega_n = 2 \times 10^{15} \text{ rad s}^{-1}$, which also corresponds to the super-current plasma frequency ω_s at $T = 0$. At intermediate temperatures these frequencies are determined by changes in the densities of superconducting and normal electrons according to the Gorter–Casimir relation. Additionally, τ is derived from the published experimental temperature dependence of the scattering rate of quasiparticles for $\text{YBa}_2\text{Cu}_3\text{O}_7$ films [18]. At the critical temperature we have $\tau_c = 1/\gamma_c = 3.57 \times 10^{-14} \text{ s}$, while the experimental temperature dependence of the scattering rate can be accurately fitted by a curve of the form

$$\gamma(t) = \gamma_c \frac{t}{(1 + a t(t^{-\xi} - 1))},$$

where a and ξ are the fitting parameters, and $t = T/T_c$. In our model we use $a = 10$ and $\xi = 1.5$. The dielectric constant of silver is also calculated using the Drude model with a plasma frequency $\omega_n = 2\pi \times 2.18 \times 10^{15} \text{ rad s}^{-1}$ and scattering time $\tau = 2.297 \times 10^{-13} \text{ s}$ [19]. The propagation of the electromagnetic modes in the gap waveguide is modeled using the three-dimensional Maxwell equations solver COMSOL Multiphysics.

The results of our simulations are presented in figures 1(c) and (d). Quite remarkably, the superconducting waveguide supports a mode that is different from the usual TEM mode existing between two perfectly conducting plates. It has the component of electric field parallel to the propagation direction (TM mode) and is therefore analogous to the surface plasmon waves supported by metals at optical frequencies. At 1 THz this mode has a wavelength several times shorter than in free space (good for miniaturization) and can propagate in a 50 nm wide gap without significant attenuation for tens of millimeters (see figure 1(d)). In comparison, a TM mode of the same frequency in a silver waveguide of identical geometry is damped within a distance of just one wavelength (figure 1(c)).

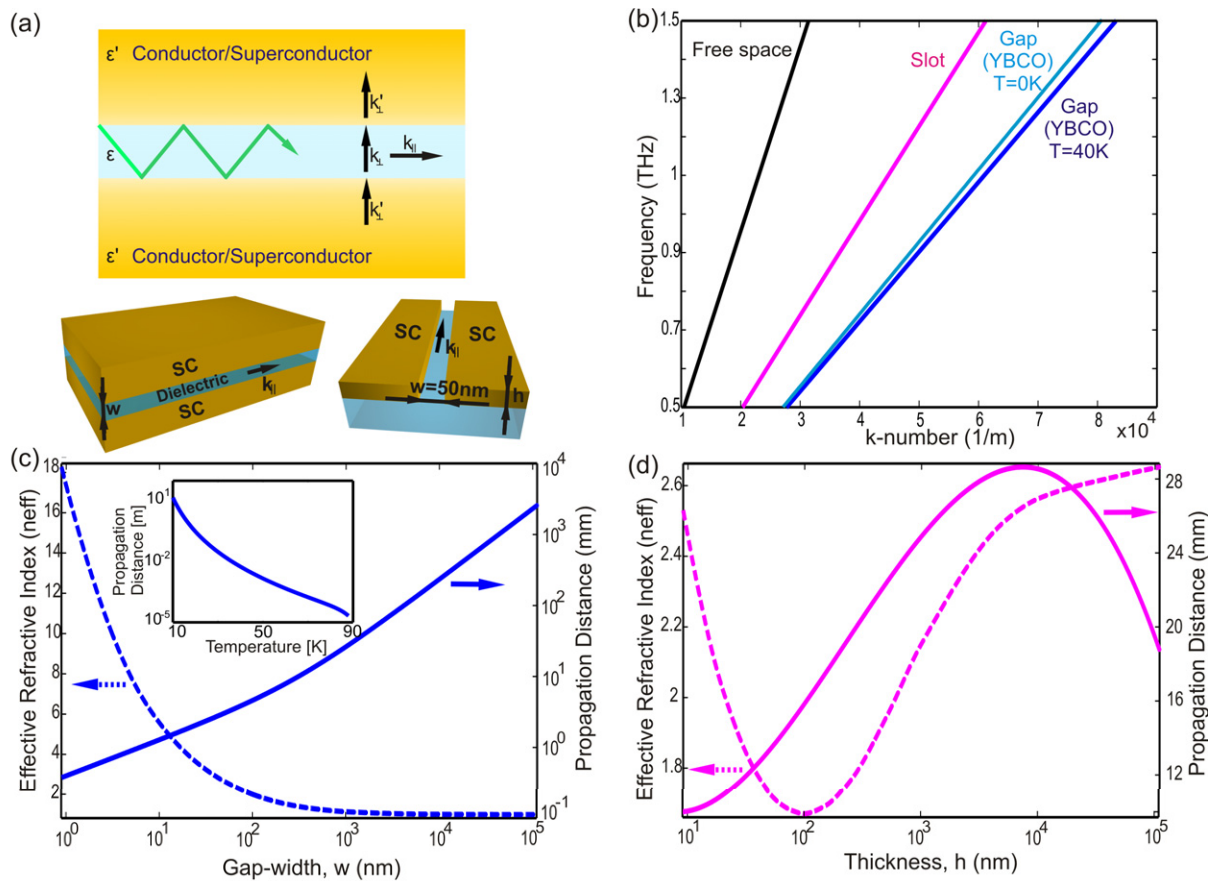


Figure 2. Dispersion and propagation characteristics of superconducting YBCO plasmonic waveguides at 40 K. (a) Schematics of the waveguide configurations used for the analytical model (top) and simulations (bottom). (b) Dispersion curves calculated for the terahertz modes propagating in free-space (black) and superconducting gap (blue) and slot (magenta) waveguides. The light blue curve represents the mode dispersion in the superconducting gap waveguide calculated analytically (superconductor at 0 K). (c) Effective refractive index (dotted curve) and propagation distance (solid curve) of the gap-plasmon calculated at 1 THz as a function of the gap width, w . The inset shows the plasmon propagation distance as a function of waveguide temperature calculated for $w = 50$ nm. (d) Effective refractive index (dotted curve) and propagation distance (solid curve) of the slot-plasmon calculated at 1 THz as a function of the superconducting film thickness, h .

Such a dramatic difference between nanoscale waveguiding efficiencies in the superconducting and the normal-conduction regimes can be explained by a simple analytical model. Consider a nanometer-sized dielectric slab embedded in either a conductor or a superconductor (see figure 2(a)). At terahertz frequencies and below, the relative permittivity of both types of host material, ϵ' , is extremely large compared to that of the slab, ϵ (i.e. $|\epsilon'/\epsilon| \gg 1$). Also, given that the thickness of the slab d is in the nanometer range, $kd \ll 1$, where k is the

light wave vector inside the dielectric. Guided modes of the dielectric slab are then defined by the Fabry–Perot condition

$$1 - r^2 \exp(2i k_{\perp} d) = 0, \quad (2)$$

where $r = (\varepsilon' k_{\perp} - \varepsilon k'_{\perp}) / (\varepsilon' k_{\perp} + \varepsilon k'_{\perp})$ is the Fresnel reflection coefficient of the interface between the superconductor/metal and the dielectric, and k_{\perp} and k'_{\perp} are the wave vector components normal to the interface in the dielectric slab and in the host material, respectively. Equation (2) is the condition for a wave to be in-phase after an up-and-down excursion across the slab, including reflections at both slab interfaces. Given this condition and the assumptions made, the propagation wave vector of the only mode supported by the gap-waveguide configuration can be expressed as

$$k_{\parallel} = \sqrt{k^2 - k_{\perp}^2} \approx k \sqrt{1 + \frac{2i}{k d \sqrt{\varepsilon'/\varepsilon}}}. \quad (3)$$

Since both d and ε' appear in a single denominator in equation (3), the value of k_{\parallel} can be significantly different from k even in the case of an air gap ($\varepsilon = 1$). If ε' is real and negative (which is a good approximation for the superconductors), k_{\parallel} is also real. In normal conductors ε' is dominated by its imaginary part and therefore gives rise to a large imaginary part in k_{\parallel} , which hinders mode propagation in the gap. Furthermore, $\text{Im}[k_{\parallel}]$ increases with decreasing gap size, thus rendering metals completely incapable of nanoscale waveguiding at low frequencies (see the [appendix](#) for details).

Low-loss superconducting waveguides are a promising solution for large-bandwidth terahertz and sub-terahertz plasmonic circuits. They offer key advantages characteristic of the plasmonic regime, such as strong lateral confinement and longitudinal compression necessary for high-density integration, but without dissipative losses that hamper plasmonic applications at optical frequencies. As an added bonus, superconducting plasmonic waveguides enable higher bandwidth and faster data transfer rates due to their extremely weak dispersion. This is demonstrated below for superconducting YBCO at 40 K for both gap- and slot-waveguide configurations (see figure 2(a)). The characteristics of the gap mode are obtained from the analytical form of its dispersion equation, which is solved using the algorithm described in [20]. The dispersion of the slot mode, as well as its effective refractive index and propagation distance, are retrieved from the results of COMSOL simulations.

Figure 2(b) shows dispersion curves calculated in the 0.5–1.5 THz range of frequencies for the modes propagating in 50 nm wide gap and slot waveguides. Similar to free-space propagation in air, the dispersion of the bounded superconducting plasmons here appears to be linear, effectively corresponding to free-space propagation in denser dielectrics. The slope of the dispersion curves can be decreased further by increasing the refractive index of the guiding regions, but more importantly, the longitudinal compression of the modes can be efficiently controlled by the size of the cross-section and the temperature of the waveguides. As is clear from figure 2(c), the effective refractive index of the plasmonic mode in the gap waveguide monotonically increases with decreasing gap size and can reach a value of 5 for a gap as large as 10 nm. Similar to optical plasmons, superconducting plasmons are also subject to the trade-off between confinement and propagation distance. However, considering a nanoscale confinement that was so far exclusive of optical plasmons, the propagation distance of its

superconducting counterpart at 1 THz extends here to a colossal value of 6.5 mm (about 60 effective wavelengths). Interestingly, the propagation distance is significantly affected by the temperature of the waveguide and can be in the range of meters near 10 K, while it drops to just a fraction of the guided wavelength near the critical temperature, as illustrated in the inset to figure 2(c). For the slot waveguide configuration (which is technologically more appealing), the plasmonic mode is confined laterally in two dimensions, and the dependences of its refractive index and propagation distance on the parameters of the waveguide cross-section are more complex (see figure 2(d)). For example, the effective refractive index of the mode residing in a 50 nm wide slot reaches a minimum value of 1.67 for a superconducting film thickness of 100 nm. The propagation distance of the plasmonic mode in such a waveguide at 1 THz is of the order of a few tens of millimeters, which corresponds to an impressive value of 100 effective wavelengths.

Obviously, we will be able to speak about plasmonics as a data handling and processing paradigm in the same way as we speak about photonics only when efficient techniques for active manipulation of plasmon signals are identified [21]. In this respect, superconductors have another important advantage over metals: the electromagnetic characteristics of superconductors may be readily altered (especially close to their critical temperature) by external stimuli such as magnetic fields, optical illumination, surface currents or heat. This opens up a new path toward ‘active plasmonic’ applications when the plasmon signal can be efficiently controlled in data processing and interconnect applications.

In essence, high-temperature superconducting waveguides constitute a promising avenue for developing ultra-compact terahertz data processing circuits, providing a superior alternative to sub-millimeter metal single-wire transmission lines and circular waveguides [22–24]. Also, propagation distances of up to several meters and truly nanoscale confinement of the guided terahertz plasmonic modes, which can be actively manipulated through various easy-to-implement routes, make the superconducting waveguides superior to other possible terahertz waveguiding solutions based on the use of semiconductors, corrugated metal surfaces or graphene. Indeed, although semiconductors can exhibit plasmonic behavior in the range of 1–10 THz with lower losses compared to metals, their conductance and kinetic inductance are both still substantially lower than in superconductors, resulting in shorter mode propagation length and weaker confinement. For example, for a semiconductor such as InSb, which has one of the lowest scattering rates of all the III–IV compounds with $\varepsilon = -14 - i12$ [25], the propagation length of a surface-guided plasmon wave at 1 THz is only 1.3 mm (around four effective wavelengths), whereas its field extends into vacuum for more than 0.18 mm. If YBCO were replaced with InSb in the gap waveguide configuration, the propagation distance of the gap mode would be $6.4 \mu\text{m}$, only a fraction of the mode effective wavelength of $14.4 \mu\text{m}$. Corrugated metal surfaces can, in principle, guide terahertz waves in the form of the so-called spoof plasmons [26, 27], but they offer no means of active control, whereas the scale of the mode localization is much larger than in the superconducting waveguides (typically tens of microns). And the efficiency of waveguides based on graphene, which has been shown to support plasmonic excitations at terahertz frequencies [28], can be severely limited by imperfections in the actual samples [29].

Finally, we would like to point out that the cryo-cooling requirement for the superconducting waveguides is no longer a serious technological limitation, as compact cryogenic devices are now widely deployed in telecommunications and sensing equipment.

Acknowledgments

This work is supported by the Royal Society and the UK's Engineering and Physical Sciences Research Council through the Nanostructured Photonic Metamaterials Programme Grant and Career Acceleration Fellowship (VAF). FJGdA acknowledges support from the Spanish MEC (MAT2010-14885 and Consolider Nanolight.es).

Appendix. Dispersion characteristics of the gap-waveguide mode

We consider a dielectric slab buried into either a conductor or a superconductor (gap waveguide), and assume that $|\varepsilon'/\varepsilon| \gg 1$ and $kd \ll 1$, where ε' is the permittivity of the conductor/superconductor, ε is the permittivity of the dielectric slab, d is the thickness of the slab and k is the light wave vector inside the dielectric. The guided modes are defined by the Fabry–Perot condition for waves traveling up and down the slab and reflecting from both interfaces, as shown in figure 2(a):

$$1 - r^2 \exp(2ik_{\pm}d) = 0, \quad (\text{A.1})$$

where

$$r = (\varepsilon'k_{\perp} - \varepsilon k'_{\perp}) / (\varepsilon'k_{\perp} + \varepsilon k'_{\perp}) \quad (\text{A.2})$$

is the TM Fresnel reflection coefficient for the interface between the superconductor/conductor and the dielectric, $k_{\perp} = (k^2 - k_{\parallel}^2)^{1/2}$ and $k'_{\perp} = (k^2 \varepsilon'/\varepsilon - k_{\parallel}^2)^{1/2}$ are the wave vector components normal to the interface in the dielectric slab and superconductor/conductor, and k_{\parallel} is the wave vector component parallel to the interface.

Equation (A.1) reflects the fact that the wave must be in-phase after one round trip in the dielectric slab, including reflections at the upper and lower interfaces. Under the approximations made we can write $k'_{\perp} \approx k(\varepsilon'/\varepsilon)^{1/2}$ and simplify expression (A.2) as

$$r \approx \left(1 - \frac{k}{k_{\perp}\sqrt{\varepsilon'/\varepsilon}}\right) / \left(1 + \frac{k}{k_{\perp}\sqrt{\varepsilon'/\varepsilon}}\right) \approx 1 - \frac{2k}{k_{\perp}\sqrt{\varepsilon'/\varepsilon}}. \quad (\text{A.2a})$$

Substituting (A.2a) into equation (A.1), we obtain

$$1 - \frac{4k}{k_{\perp}\sqrt{\varepsilon'/\varepsilon}} \approx 1 - 2ik_{\perp}d, \quad (\text{A.3})$$

so that

$$k_{\perp} \approx \sqrt{\frac{-2ik}{d\sqrt{\varepsilon'/\varepsilon}}}. \quad (\text{A.3a})$$

From (A.3a) the wave vector component parallel to the interface can be obtained in the form

$$k_{\parallel} = \sqrt{k^2 - k_{\perp}^2} \approx k \sqrt{1 + \frac{2i}{kd\sqrt{\varepsilon'/\varepsilon}}}. \quad (\text{A.4})$$

Expression (A.4) is valid if $|\varepsilon'/\varepsilon| \gg 1$ and $kd \ll 1$. Since these two conditions affect the same denominator in (A.4), k_{\parallel} can be either very close to or different from k . We consider two limiting cases:

- (i) The ideal superconductor ($T \rightarrow 0$)

In this case $\varepsilon' \sim -\omega_s^2/\omega^2$ with $\omega = \omega_s$, which immediately leads to

$$k_{\parallel} \approx k \sqrt{1 + \frac{2(\omega/\omega_s)\sqrt{\varepsilon}}{kd}}. \quad (\text{A.4a})$$

Expression (A.4a) reflects the fact that the mode propagates in an ideal superconducting gap waveguide without losses (k_{\parallel} is real) and its dispersion can significantly deviate from the light line for small d (stronger confinement).

- (ii) The ideal conductor ($\omega \rightarrow 0$)

In this case $\varepsilon' \sim i\omega_n^2\tau/\omega$, which leads to

$$k_{\parallel} \approx k \sqrt{1 + \frac{2(\omega/\omega_n)}{kd} \sqrt{\frac{i\varepsilon}{\omega\tau}}}. \quad (\text{A.4b})$$

Thus, there are significant losses for the mode propagating in an ideal conducting gap waveguide, and the level of losses increases with the departure of k_{\parallel} from the light line, i.e. when the mode is subjected to stronger confinement (d decreases).

References

- [1] Bromgersma M L and Shalaev M 2010 *Science* **328** 440
- [2] Zheludev N I 2010 *Science* **328** 582
- [3] Soukoulis C and Wegener M 2010 *Science* **330** 1633
- [4] Boltasseva A and Atwater H A 2010 *Science* **331** 290
- [5] Mooij J E and Schon G 1985 *Phys. Rev. Lett.* **55** 114
- [6] Fertig H A and Das Sarma S 1990 *Phys. Rev. Lett.* **65** 1482
- [7] Golick V A, Kadygrob D V, Yampol'skii V A, Rakhmanov A L, Ivanov B A and Nori F 2010 *Phys. Rev. Lett.* **104** 187003
- [8] Buisson O, Xavier P and Richard J 1994 *Phys. Rev. Lett.* **73** 3153
- [9] Ricci M, Orloff N and Anlage S M 2005 *Appl. Phys. Lett.* **87** 034102
- [10] Fedotov V A, Tsiatmas A, Shi J H, Buckingham R, de Groot P, Chen Y, Wang S and Zheludev N I 2010 *Opt. Express* **18** 9015
- [11] Katterwe S-O, Motzkau H, Rydh A and Krasnov V M 2010 arXiv:1010.6172
- [12] Gu J, Singh R, Tian Z, Cao W, Xing Q, He M, Zhang J W, Han J, Chen H-T and Zhang W 2010 *Appl. Phys. Lett.* **97** 071102
- [13] Singh R, Xiong J, Azad A K, Yang H, Trugman S A, Jia Q X, Taylor A J and Chen H-T 2012 *Nanophotonics* **1** 117
- [14] Tsiatmas A, Buckingham A R, Fedotov V A, Wang S, Chen Y, de Groot P A J and Zheludev N I 2010 *Appl. Phys. Lett.* **97** 111106
- [15] Tian Z, Singh R, Han J, Gu J, Xin Q, Wu J and Zhang W 2010 *Opt. Lett.* **35** 3586
- [16] Gorter C J and Casimir H B G 1934 *Phys. Z.* **35** 963
- [17] Majedi A 2004 *IEEE Trans. Appl. Supercond.* **19** 907
- [18] Gao F, Kruse J W, Platt C E, Feng M and Klein M V 1993 *Appl. Phys. Lett.* **63** 2274
- [19] Israelachvili J N 1992 *Intermolecular and Surface Forces* (New York: Academic)

- [20] Kekatpure R D, Hryciw A C, Bernard E S and Brongersma M L 2009 *Opt. Express* **17** 24112
- [21] MacDonald K F and Zheludev N I 2010 *Laser Photon. Rev.* **4** 562
- [22] McGowan R W, Gallot G and Grischkowsky D 1999 *Opt. Lett.* **24** 1431
- [23] Wang K and Mittleman D M 2004 *Nature* **432** 376
- [24] Akalin T 2006 *IEEE Trans. Microw. Theory Tech.* **54** 2762
- [25] Palik E D 1998 *Handbook of Optical Constants of Solids* vol 3 (New York: Academic)
- [26] Ulrich R and Tacke M 1973 *Appl. Phys. Lett.* **22** 251
- [27] Rivas J G 2008 *Nature Photon.* **2** 137
- [28] Ju L, Geng B, Horng J, Girit C, Martin M, Hao Z, Bachtel H A, Liang X, Zettl A, Shen Y R and Wang F 2011 *Nature Nanotechnol.* **6** 630
- [29] Jablan M, Buljan H and Soljagic M 2009 *Phys. Rev. B* **80** 245435